PLOS ONE

RESEARCH ARTICLE

Epiphytic diatom community structure and richness is determined by macroalgal host and location in the South Shetland Islands (Antarctica)

Andrea M. Burfeid-Castellanos[1]*, Rafael P. Martín-Martín[2], Michael Kloster[1], Carlos Angulo-Preckler[3], Conxita Avila[4], Bánk Beszteri[1]

1 Universität Duisburg-Essen, Phycology, Essen, Germany, **2** Laboratory of Botany, Faculty of Pharmacy and Food Science, University of Barcelona (UB), Barcelona, Spain, **3** Norwegian College of Fishery Science, UiT, The Arctic University of Norway, Tromsø, Norway, **4** Faculty of Biology, Department of Evolutionary Biology, Ecology, and Environmental Sciences, and Institute of Biodiversity Research (IrBIO), Universitat de Barcelona, Barcelona, Catalonia

* andrea.burfeid-castellanos@uni-due.de

Citation: Burfeid-Castellanos AM, Martín-Martín RP, Kloster M, Angulo-Preckler C, Avila C, Beszteri B (2021) Epiphytic diatom community structure and richness is determined by macroalgal host and location in the South Shetland Islands (Antarctica). PLoS ONE 16(4): e0250629. https://doi.org/10.1371/journal.pone.0250629

Editor: Judi Hewitt, University of Waikato, NEW ZEALAND

Received: November 30, 2020

Accepted: April 10, 2021

Published: April 30, 2021

Peer Review History: PLOS recognizes the benefits of transparency in the peer review process; therefore, we enable the publication of all of the content of peer review and author responses alongside final, published articles. The editorial history of this article is available here: https://doi.org/10.1371/journal.pone.0250629

Data Availability Statement: All image files are available from the PANGAEA database (https://doi.pangaea.de/10.1594/PANGAEA.925913). All code

Abstract

The marine waters around the South Shetland Islands are paramount in the primary production of this Antarctic ecosystem. With the increasing effects of climate change and the annual retreat of the ice shelf, the importance of macroalgae and their diatom epiphytes in primary production also increases. The relationships and interactions between these organisms have scarcely been studied in Antarctica, and even less in the volcanic ecosystem of Deception Island, which can be seen as a natural proxy of climate change in Antarctica because of its vulcanism, and the open marine system of Livingston Island. In this study we investigated the composition of the diatom communities in the context of their macroalgal hosts and different environmental factors. We used a non-acidic method for diatom digestion, followed by slidescanning and diatom identification by manual annotation through a web-browser-based image annotation platform. Epiphytic diatom species richness was higher on Deception Island as a whole, whereas individual macroalgal specimens harboured richer diatom assemblages on Livingston Island. We hypothesize this a possible result of a higher diversity of ecological niches in the unique volcanic environment of Deception Island. Overall, our study revealed higher species richness and diversity than previous studies of macroalgae-inhabiting diatoms in Antarctica, which could however be the result of the different preparation methodologies used in the different studies, rather than an indication of a higher species richness on Deception Island and Livingston Island than other Antarctic localities.

Introduction

On Antarctic coasts, marine macro- and microalgae in ice and benthos are the main primary producers [1]. When free of shelf-ice, these benthic producers can account for up to 90% of

and datafiles are accessible at DRYAD database (https://doi.org/10.5061/dryad.ngf1vhhsm).

Funding: Samples were collected in the frame of the DISTANTCOM (Diversity and Structure of benthic Antarctic communities, CTM2013-42667/ANT) and BLUEBIO (Bioactive marine natural products in our environmentally changing planet, CTM2016-78901) grants funded by the Spanish Government (CA). The Deutscher Akademischer Austauschdienst (DAAD) funded ABC with a short-term grant (57442045, grant number 91673491). We also acknowledge support by the Open Access Publication Fund of the University Duisburg-Essen.

Competing interests: The authors have declared that no competing interests exist.

the total net primary production of the ecosystem [1]. The surface of macroalgal hosts also serves as habitat for benthic microalgae (mainly diatoms) in the Antarctic and Subantarctic regions. Although macroalgae cannot be interpreted either as synonymous with or part of plants in the systematic sense, these macroalgae-inhabiting diatom assemblages are usually referred to as "epiphytic" in the literature [2–4]. This association provides a basis for complex ecological interactions between diatoms and macroalgal hosts, which are only partially understood [5]. It is known that epiphytic diatoms can facilitate the adherence of other organisms to any substrate [6]. Epiphytic diatoms and other biofouling organisms can also reduce light intensity available to the host algae [7]. Interactions with surface-inhabiting diatoms can influence the performance of macro- and microalgae species to acclimate or adapt to new ecosystem pressures like climate change [8,9] or invasive species from lower latitudes [10,11].

Previous studies on macroalgae- inhabiting diatoms have focussed on the taxonomic composition and ecology of the epiphytic diatom flora on macroalgae around Antarctica [2,3,5,12–15] or terrestrial habitats [16]. Some studies focussed on the floristics and ecology of taxonomically diverse hosts at a single location, constructing a flora of Vestfold Hills [12] and King George's Island Potter Cove [2] respectively. Majewska et al. took a different approach by characterizing the epiphytic diatom ecology and flora of a small number of host taxa [3,13–15] across different locations [15].

In this study, diatom communities collected from diverse algal hosts belonging to different classes from two islands of the South Shetland archipelago, Deception (DI) and Livingston Islands (LI), were investigated. These islands differ strongly in their geology and geomorphology: DI is an active volcano, with comparatively young coastal ecosystems that undergo thermal disturbance due to volcanic activities on an irregular basis [17]. In contrast, LI harbours relatively undisturbed, pristine coastal locations with very steep inner slope moraines [18]. We attempt to interpret differences in epiphytic diatom compositions in a framework of environmental sorting effects resulting from differences in abiotic environments (island geology / coastline ecology, including depth), biotic interactions with macroalgal hosts (host phylogenetic position and/or gross morphology) and of a presumably low, but perhaps not negligible dispersal limitation in shaping these diatom communities. Although limited sampling in this distant region affects our study and limits the causal interpretability of statistical comparisons, just as it does for similar investigations in general, we attempt to disentangle the correlative contribution of these factors to community differences, while also substantially extending our diatom floristic knowledge of the Antarctic region.

Materials and methods

A total of 36 macroalgal samples from 20 species and 2 macroscopically visible diatom community samples, i.e. diatom blooms attached to a substrate and visible to the naked eye, were taken in three consecutive annual expeditions (2017–2019) to the Antarctic South Shetland Islands, namely Deception (DI) and Livingston Island (LI) (Fig 1). The macroalgal samples were collected by hand from the intertidal range, as well as by snorkelling or by SCUBA divers at subtidal depths (Table 1). Simultaneously, temperature measurements were taken. All sampling permits (CPE-EIA-2013-7, CPE-EIA-2015-7, and CPE-EIA-2017-7) were issued by the Spanish Polar Committee within the Antarctic projects DISTANTCOM and BLUEBIO (CTM2013-42667/ANT and CTM2016-78901).

Macroalgae were obtained simultaneously with other benthic organisms at each sampling spot and pooled together in 1L receptacles, keeping different algal species separated from each other. At the wet lab, the specimens were sorted by *phylum* and identified to lowest taxon, usually species, following literature [19,20]. The species samples of one sampling site and day were

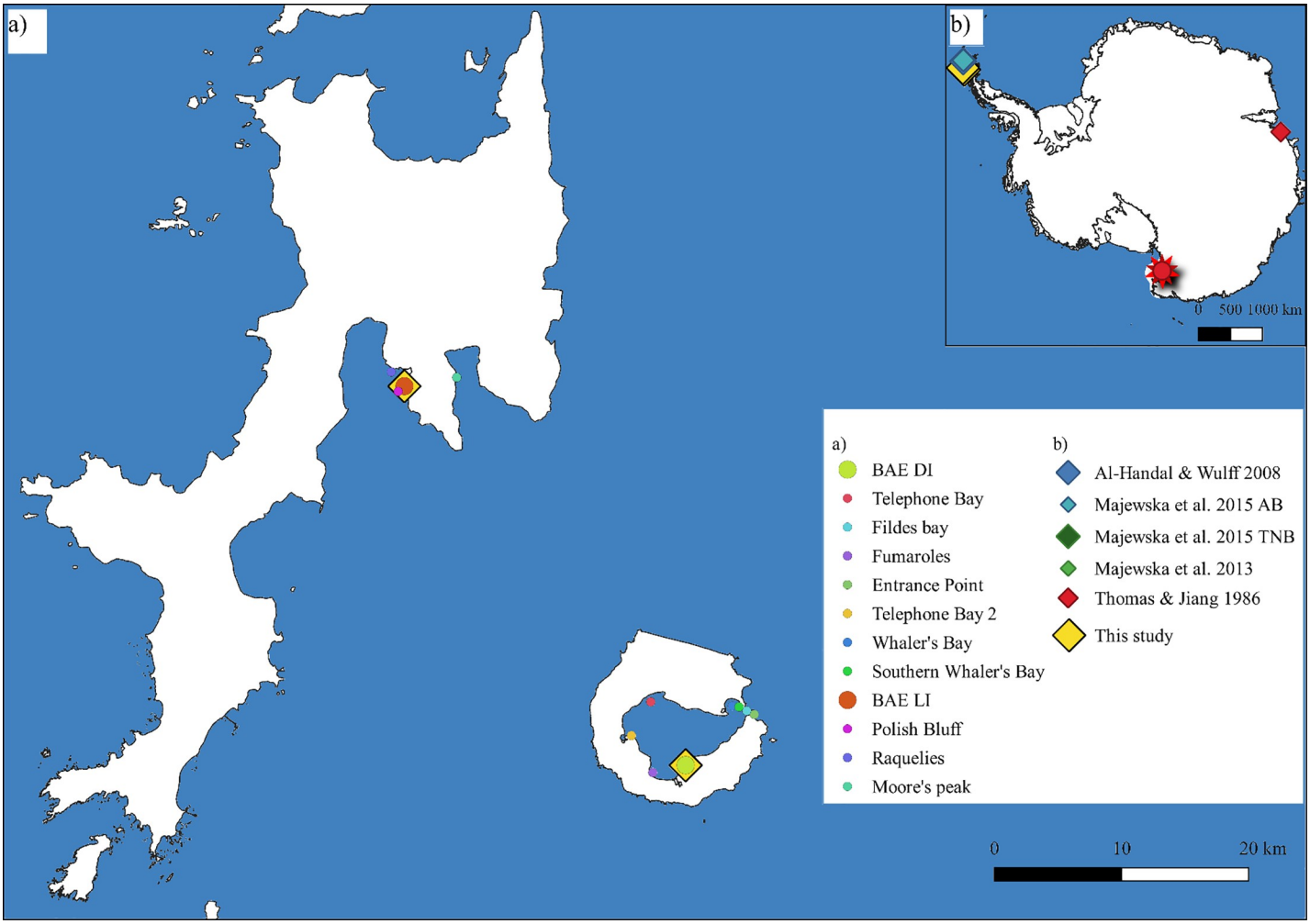

Fig 1. Sampling localities. a) Distribution of sampling sites in Livingston (LI) and Deception Islands (DI). b) sampling sites from previous studies from the literature. The yellow rectangle in b) shows the location of LI and DI. Map constructed with QGIS software.

https://doi.org/10.1371/journal.pone.0250629.g001

kept in separate zip-style bags and frozen at -20˚C until further processing at the University of Barcelona. The macroalgal attributes of branching pattern, based on thallus morphology, and age, meaning the annuality of macroalgae (annual, biannual or pluriannual) of each species, were ascertained according to literature e.g. [19,21,22]. Epiphytic diatoms were extracted under laboratory conditions using a small part of the macroalgae, an overall appraisal of epiphyte incidence was made before scraping the surface into the receptacle with 80–100 ml of water depending on epiphyte density. The algae were also immersed and the samples were centrifuged [e.g. 23]. After this, the macroalgal part was extracted again for further use. Depending on epiphyte concentration, several aliquots were made and fixated using ethanol.

Diatoms were washed in distilled water to reduce remaining salinity. Samples were homogenized and centrifuged at 1000 rpm (Eppendorf centrifuge 5810 R, Eppendorf AG, Germany) for five minutes, and again filled up with deionized water. This procedure was repeated five times. Diatoms were prepared using the Friedrichs' [24] variation of Carr et al.'s method [25], using ten times diluted bleach (Domol Hygiene Reiniger, AGB Rossmann GmbH), based on 5% sodium hypochlorite as the undiluted oxidizing agent, with a treatment period of 30–45 min depending on the amount of organic matter present in the sample. The thus cleaned

Table 1. Sample descriptions: Number of samples, replicates and macroalgal hosts.

	Host class	Host thallus morphology	Host annuality	Number of diatom taxa found (genera)	Number of samples (replicates)	Depth [m]	Year	Island
***Adenocystis utricularis* (Bory) Skottsberg)**	Phaeo	Sac, Unb	A	47 (22)	1 (2)	0	2018	LI
***Ballia callitricha* (C. Agardh) Kützing**	Rhodo	Fil, Bra	A, B	41 (14)	1	22.1	2018	DI
***Berkeleya rutilans* (Trenthepohl ex Roth) Grrunow**	Bacill.	Fil	A	16 (7)	1	4.5	2017	DI
***Cystosphaera jacquinotii* (Montagne) Skottsberg**	Rhodo	Lam, Bra	P	25 (9)	1	27	2017	DI
***Delisea pulchra* (Greville) Montagne**	Rhodo	Fil, Bra	P	50 (16)	4	21–23.4	2018, 2019	LI
***Desmarestia anceps* Montagne**	Phaeo	EBT	P	44 (16)	3	0–22	2017	DI
***D. antarctica* R. L. Moe & P. C. Silva**	Phaeo	EBT	P	57 (24)	2	0–13	2017, 2018	DI, LI
***Desmarestia* sp J. V. Lamouroux**	Phaeo	EBT	P	18 (5)	1	25	2017	DI
***Gigartina skottsbergii* Setchell & N. L. Gardner**	Rhodo	Lam, Bra	A,B	53 (17)	3	5.5–23.4	2017–19	DI, LI
***Gymnogongrus cf. turquettii* Hariot**	Rhodo	Lam, Bra	A, B	47 (11)	2	23–23.4	2018, 2019	LI
***Himantothallus grandifolius* (A. Gepp & E.S. Gepp) Zinova**	Phaeo	Lam, Unb	P	50 (18)	3	23–25	2017, 2018	DI, LI
***Iridaea cordata* (Turner) Bory**	Rhodo	Lam, Unb	A, B	46 (15)	3	0–25	2017, 2018	DI, LI
***Monostroma hariotii* Gain**	Chloro	Lam, Bra	A, B	16 (7)	1	23	2018	LI
***Myriogramme manginii* (Gain) Skottsberg**	Rhodo	Lam, Bra	Pp	32 (11)	1	22.1	2018	LI
***Palmaria decipiens* (Reinsch) R. W. Ricker**	Rhodo	Lam	Pp	55 (23)	3	2–17.5	2017, 2018	DI, LI
***Picconiella plumosa* (Kylin) J. De Toni**	Rhodo	BT	A, B	40 (13)	1	22.1	2018	LI
***Plocamium cartilagineum* (Linnaeus) P.S. Dixon**	Rhodo	EBT	A, B	50 (15)	4	22.1–25	2018, 2019	LI
***P. cf. hookeri* Harvey**	Rhodo	EBT	A, B	23 (5)	1	20	2018	LI
***Pyropia endiviifolia*(A.Gepp & E.Gepp) H.G.Choi & M.S.Hwang**	Rhodo	Lam	A, B	39 (13)	1	23	2018	LI
***Brandinia mosimanniae* L.F. Fernandes & L. K. Procopiak [macroscopic]**	Bacill.	Fil	A	33 (17)	1	8.2	2018	DI
In total				131(85)	38	0–25	2017–2019	DI, LI
In total (macroalgae)				120 (47)	36	0–25	2017–2019	DI, LI

Class names: Phaeo = Phaeophyceae, Rhodo = Rhodophyta, Chloro = Chlorophyta, Bacill = Bacillariophyceae. Sampling sites: LI = Livingston Island, DI = Deception Island. Morphological trends: EBT = Erect Branched Thallus, BT = Branched Thallus, Sac = Saccular Thallus, Fil = Filament, Lam = Laminar Thallus, Bra = Branched, Unb = Unbranched. Annual trends: P = Perennial, Pp = Pseudoperennial, B = Biannual, A = Annual.

https://doi.org/10.1371/journal.pone.0250629.t001

diatom frustules were washed five times following the same procedure as before the bleach treatment. The frustule suspensions were then dripped onto coverslips, left to dry, quality checked and mounted using Norland Optical Adhesive 61 (refraction index = 1.56, Norland Products Inc., Cranbury, New Jersey, US).

Slide scanning methodology was modified after Kloster et al. [26] using a Metafer 4 slide scanner system (MetaSystems, Altlussheim, Germany) attached to an Axio Imager.Z2 microscope (Carl ZEISS AG, Oberkochen, Germany). The scans were made with a 63x objective

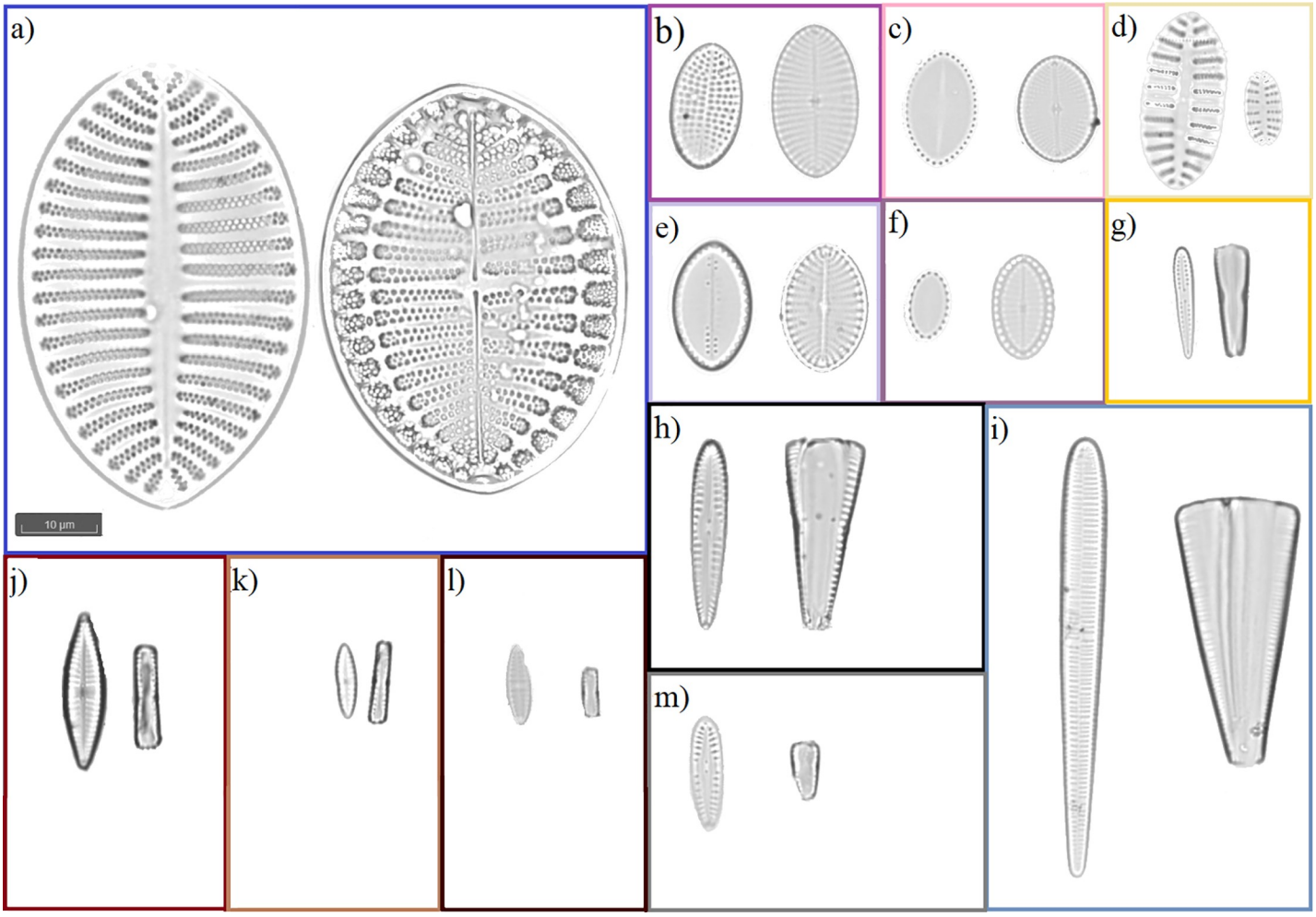

Fig 2. Predominant diatoms found on Antarctic macrophytes. Monoraphid diatoms shown in raphe and raphe-less valve view. Biraphids shown in valvar and pleural view. a) *Cocconeis fasciolata*, b) *Cocconeis californica var. californica*, c) *Cocconeis dallmannii*, d) *Cocconeis sp. 1*, e) *Cocconeis californica var. kerguelensis*, f) *Cocconeis melchioroides*, g) *Gomphonemopsis cf. ligowskii*, h) *Pseudogomphonema kamtschaticum*, i) *Licmophora gracilis*, j) *Navicula glaciei*, k) *Navicula incertata*, l) *Navicula perminuta*, m) *Pseudogomphonema sp. 1*.

https://doi.org/10.1371/journal.pone.0250629.g002

(Zeiss Plan-Apochromat 1.4 with oil immersion) for an area of 54 x 75 visual fields, resulting in 4,050 images per slide, covering an area of 42.5 mm^2. For each field of view, images at 80 different focus levels were taken and combined to extended focus images. For the resulting images 980 pixels equal 100 µm, (e. g. see Fig 2 and images available in PANGAEA: https://doi.pangaea.de/10.1594/PANGAEA.925913.

The 4,050 extended focus depth images depicting each sample slide were stitched together to a virtual slide image using the Fiji image processing software [27]. First, the MIST plug-in [28–30] was used to calculate the exact relative position of the individual field of view-images. Subsequently, the tool MIST converter (Kloster, unpublished) was used to subdivide the slide into 3 segments of not more than 2 GB each and to process the position data for the last step, which utilized Grid / collection stitching ImageJ plug-in [31] for composing the virtual slide images. For each slide, this resulted in three virtual slide images which were then uploaded into the web-based annotation tool BIIGLE 2.0 [32].

In BIIGLE, the "random sampling" function was used to manually examine up to 400 randomly distributed sections of each virtual slide image at high magnification. Diatoms

contained within these sections were identified manually until ca. 500 identified specimens were reached for each sample, which mostly was the case during analysing the first of the three virtual slide image segments. In two instances material density on the slide was too low to allow for 500 annotations even after examining all three image segments comprising the sample, but the number of results was deemed sufficient to account for statistical significance. Diatoms were identified using epiphyte specific (e. g. [2,3,13–15]) and general [33,34] taxonomic bibliography to the lowest possible level. For each diatom specimen identified in this procedure, also their position (valvar vs. pleural view) and the presence of teratologic deformations was recorded. Teratologies refer to malformations, i.e. deviations from usual species-specific outline form or valve pattern, that can occur as a result of biotic and abiotic stresses [35].

Once all slides were identified, diatom inventories per virtual slide image were downloaded and, in cases where multiple images for the same slide were annotated, their counts were combined. The resulting inventories were turned into relative abundances (%). We calculated species richness and Shannon diversity [36]. To reduce influence of dominant taxa, relative abundances were square root transformed. Records of epiphytic diatom taxa were collated from previous studies undertaken around Antarctica (Fig 1), namely the South Shetland Islands (King George Island, in Admiralty Bay [15] and Potter Cove [2]), in McMurdo Sound (Terra-nova Bay [13–15] and Cape Evans [3]) and the Vestfold Hills (Davis Station [12]). Since the methodologies diverged in these studies and Thomas & Jiang did not provide numeric abundances, we used presence-absence data from the identified diatoms in each study. Slide scans and image cut-out of every single specimen identified in our study can be accessed in PANGAEA (https://doi.pangaea.de/10.1594/PANGAEA.925913). Statisical analyses, R Script and data matrices used are available in DRYAD (doi: https://doi.org/10.5061/dryad.ngf1vhhsm:).

Statistical analysis

All statistical analyses were made with R software version 3.6.1 [37] on RStudio version 1.2.5019 [38]. Characterization by host species, thallus morphology, and branching pattern as well as annuality was made using IndVal algorithms [39]. The differential ternary graph showing species distributions of the epiphytic diatoms between three host classes (Phaeophyceae, Rhodophyta and Chlorophyta) was made using the 'ggtern' package [40]. Most multivariate analyses (non-metric dimensional scaling–nMDS-, principal component analysis—PCA) and analysis of similarity (ANOSIM), as well as the richness and diversity measures were calculated using the package 'vegan' [41]. Similarity of percentages (SIMPER) analyses were made using PRIMER software 7.0.13 (Primer-e Quest Research Limited, Auckland, New Zealand). Iterative hierarchical clustering was performed with 'cluster' [42] and 'pvclust' [43] packages. A Mantel test was performed combining the 'geosphere' [44] and 'vegan' packages When significant (P-value < 0.05), these values were further characterized as highly significant (***, $p<0.001$), very significant (** $0.001< p < 0.01$), or significant (*, $0.01 < p <0.05$). The map in Fig 1 was constructed with QGIS software v. 3.16, [45] with the Quantarctica package (ADD_Coastline_res_line_Sliced) [46].

Results

Epiphytic diatom floristics and ecology

A total of 120 species of diatoms of 47 genera (S1 Table) were identified from 36 Antarctic macroalgae (Table 1). All macroalgae studied had varying degrees of epiphytic diatom colonization, with a range of 13 to 56 species per sample. The most frequent and predominant species of diatoms found in association with macroalgae (Fig 2) were generalist diatoms such as *Pseudogomphonema kamtschaticum* (Grunow) Medlin (up to 25% relative abundance in a

sample, present in all but one samples) or as yet undescribed species as *Navicula cf. perminuta* Grunow (up to 64% relative abundance in a sample, present in all samples) and *Pseudogomphonema* sp. 1 (up to 59% relative abundance in a sample, present in 29 samples). We recorded 19 diatom species not previously reported from these islands (S1 Table). Teratological frustules accounted for 0 to 2.3% of the counted cells. Diatoms had more teratologies on Rhodophyta (with an incidence of up to 2.4% of the sample and for 57.89% of all samples) than on Phaeophyceae (with an incidence of under 1%, in 32.89% of the samples).

Shannon diversity and diatom species richness (Table 2) did not follow a clear trend with location or depth. Neither host class nor host species was decisive for species richness. However, diatom species composition changed significantly for host class (Mantel statistic $r = 0.45^{***}$). Shannon diversity on Phaeophyceae varied in a wider range (H' = 0.97–3.03) than on Rhodophyta (H' = 1.33–2.64), macroscopically visible diatoms (H' = 0.98–1.38) or Chlorophyta (H' = 1.49). Species richness was also more variable on Phaeophyceae (S = 13–56) than on Rhodophyta (S = 13–42), Bacillariophyceae (S = 16–33) and the Chlorophyta sample (S = 16). For some macroalgae species, different individual samples had similar diversity (such as *Delisea pulchra*, H' = 1.81–2.02) but varying species richness values (S = 19–28), or the other way around, as with *Iridaea cordata* (H' = 1.51–2.35, S = 18–23). In the case of *Himantothallus grandifolius*, diversity had a very wide range (H' = 0.97–2.66) as did species richness (H' = 13–39). All rarefaction curves calculated per host were saturated (S1 Fig) and Rhodophyta had the highest species richness of all macrophytes studied.

The ternary plot illustrates the preferences between the host groups for the predominant species (Fig 3), where only *Pseudogomphonema kamtschaticum* showed no host preference at all (Fig 3). On the other hand, some diatom-macroalgae class relationships are rather specific, as *Licmophora gracilis* was found mostly on the Chlorophyta, *Cocconeis melchioroides* on Rhodophyta, and *Cocconeis fasciolata* on Phaeophyceae. The ternary plot (Fig 3) further shows that most diatom taxa were shared amongst Phaeophyceae and Rhodophyta. Since only one Chlorophyta was sampled, some or all of these might represent host generalist taxa which would also be found on Chlorophyta with more sampling effort.

ANOSIM showed that host class had the highest impact of the macroalgal characteristics on diatom distribution ($R = 0.47^{***}$). Host branching patterns ($R = 0.17^{*}$) and annuality ($R = 0.23^{***}$) also affected the diatom community to varying degrees. As the rarefaction curves (S1 Fig) show, only Phaeophyceae and Rhodophyta arrived at saturation levels with the samples explored. When comparing the diatom communities on these macroalgal classes (Phaeophyceae and Rhodophyta), only Rhodophyta had significant ANOSIM values, e.g. variation inside the class and between species (Table 3). Diatom communities growing on Rhodophyta were found to be substantially shaped by locality ($R = 0.39^{***}$), year ($R = 0.38^{***}$), and annuality of the host ($R = 0.25^{***}$).

The nMDS multivariate analysis (Fig 4) performed on diatom communities showed a small degree of differentiation depending on macroalgal host. A two-dimensional solution was sufficient due to the low stress value recorded (0.16). On the other hand, a SIMPER analysis on predominant diatoms showed very high standard deviation levels (S2 Table). When looking into the most abundantly sampled Rhodophyta and Phaeophyceae (Table 4), the SIMPER analysis results showed that *Navicula perminuta*, *Gomphonemopsis ligowskii* and *Cocconeis melchioroides* were the most significant contributors to the average dissimilarity.

Diatom distribution in Antarctica

Diatoms in the South Shetland Islands. The annual mean temperature of both islands was 2˚C, but the temperature range in DI comprised 0–4˚C (increasing even more towards the

Table 2. Sampling site characterization of depth and temperature (T) and diatom epiphyte richness (S) and diversity (H') found on each macroalgal host.

Locations	Depth (m)	T (˚C)	Macroalgal host	Species diversity (H')	S
Livingston–Raquelies	13	/	*Adenocystis utricularis*	1.76	45
Deception–Antarctic base	4.5	3	*Berkeleya rutilans*	0.98	16
Deception–Fumaroles	8.2	*	*Brandinia sp.*	1.38	33
Livingston–Moore's peak	22.1	2	*Ballia callitricha*	2.58	40
Deception–Whaler's bay	25	2	*Cystosphaera jacquinottii*	1.74	24
Livingston–Polish Bluff	21	3	*Delisea pulchra*	2.02	27
Livingston–Polish Bluff	22.1	1	*Delisea pulchra*	1.81	19
Livingston–Moore's peak	23	2	*Delisea pulchra*	1.93	20
Livingston–Polish Bluff	23.4	2	*Delisea pulchra*	2.02	28
Deception–front of base	0	/	*Desmarestia anceps*	2.17	30
Deception–front of base	0	/	*Desmarestia anceps*	1.51	13
Deception–Fildes bay	22	3	*Desmarestia anceps*	1.33	22
Livingston–Raquelies	13	2	*Desmarestia antactica*	3.03	56
Deception–Antarctic base	0	/	*Desmarestia antarctica*	1.76	17
Deception–Whaler's bay	25	2	*Desmarestia* sp	2.08	17
Deception–Seal colony	5.5	4	*Gigartina skottsbergii*	2.56	42
Livingston–Moore's peak	22.1	2	*Gigartina skottsbergii*	2.18	21
Livingston–Polish Bluff	23.4	2	*Gigartina skottsbergii*	1.34	13
Livingston–Polish Bluff	23.4	2	*Gymnogogrus turquettii*	1.77	32
Livingston–Moore's peak	23	2	*Gymnogongrus turquettii*	2.09	37
Deception–Fildes bay	25	2	*Himantothallus grandifolius*	0.97	13
Deception–Whaler's bay	25	2	*Himantothallus grandifolius*	2.66	39
Livingston–Moore's peak	23	2	*Himantothallus grandifolius*	2.05	23
Deception–front of base	0	/	*Iridaea cordata*	1.51	18
Deception–Whaler's bay	25	2	*Iridaea cordata*	2.35	23
Livingston–Moore's peak	22.1	1	*Iridaea cordata*	2.25	23
Livingston–Moore's peak	23	2	*Monostroma hariotii*	1.49	16
Livingston–Moore's peak	22.1	2	*Myriogramme cf. manguinii*	2.36	31
Deception–Drum	17.5	2	*Palmaria decipiens*	1.96	30
Deception–Telephone bay	14.1	3	*Palmaria decipiens*	1.43	30
Livingston–Antarctic Base	2	2	*Palmaria decipiens*	1.85	26
Livingston–Moore's peak	22.1	2	*Piccionella plumosa*	2.49	39
Livingston–Raquelies	25	2	*Plocamium cartilagineum*	2.18	22
Livingston–Moore's peak	22.1	1	*Plocamium cartilagineum*	2.19	30
Livingston–Moore's peak	23	2	*Plocamium cartilagineum*	2.31	30
Livingston–Polish Bluff	23.4	2	*Plocamium cartilagineum*	1.85	25
Livingston–Moore's peak	20	1	*Plocamium cf. hookerii*	2.01	23
Livingston–Moore's peak	23	2	*Pyropia endiviifolia*	2.64	38

Intertidal temperature was not recorded [/].

* Taken in the fumaroles, temperature estimated between 40–80˚C.

https://doi.org/10.1371/journal.pone.0250629.t002

fumaroles, but not recorded), and 1–3˚C in LI. A total of 15 samples came from DI (diatom epiphyte taxa n = 94) and 23 samples from LI (diatom epiphyte taxa n = 82), and 66 diatom taxa (21 genera) were shared between both islands. Diatom compositions of Rhodophyta and Phaeophyceae from DI and LI clustered together, separated from the Chlorophyta and macroscopic Bacillariophyceae samples, in hierarchical cluster analysis (distance = Euclidean,

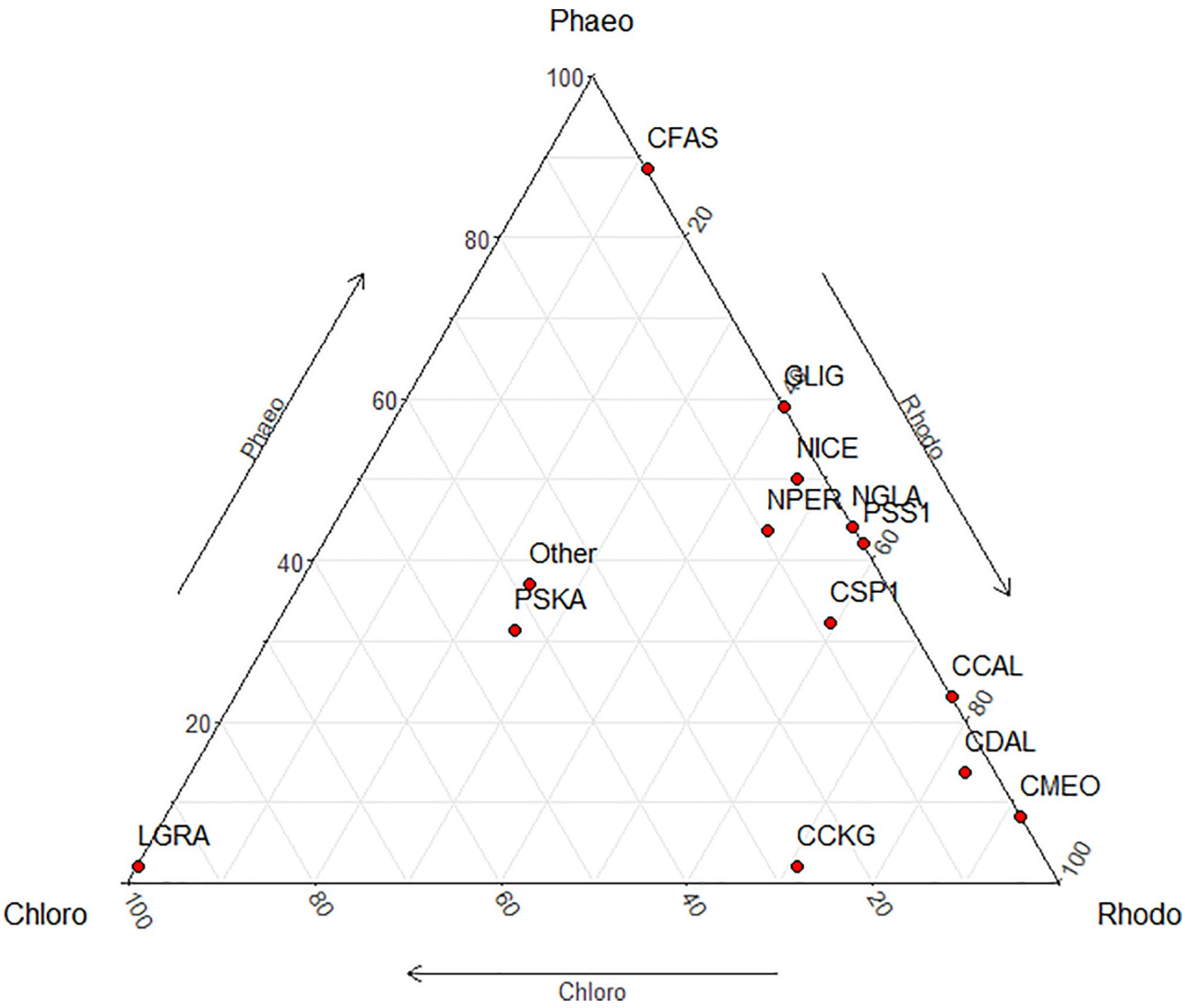

Fig 3. Ternary plot of predominant epiphytic diatoms shared between Rhodophyta (Rhodo), Phaeophyceaes (Phaeo) and Chlorophyta (Chloro). Species codes: CCAL = *Cocconeis californica*, CCKG = *Cocconeis californica var. kerguelensis*, CDAL = *Cocconeis dallmanii*, CFAS = *Cocconeis fasciolata*, CMEO = *Cocconeis melchioroides*, CSP1 = *Cocconeis sp. 1*, GLIG = *Gomphonemopsis ligowskii*, LGRA = *Licmophora gracilis*, NGLA = *Navicula glacialis*, NICE = *Navicula incertata*, NPER = *Navicula perminuta*, PSKA = *Pseudogomphonema kamtschaticum*, PSS1 = *Pseudogomphonema sp 1*, Other = diatom species in under 2% frequency and abundance.

https://doi.org/10.1371/journal.pone.0250629.g003

cluster = average linkage, bootstrap = 94%, not shown). A redundancy analysis (RDA), on the other hand, showed a separation between DI and LI communities (Fig 5). This was corroborated by the results of the Mantel test (geographical distance matrix vs. diatom communities,

Table 3. ANOSIM test results performed on communities from Phaeophyceae (Phae) and Rhodophyta (Rhod) hosts.

	Loc		Depth		Depth Int		Year		Host Morph.		Host Branch		Host Annuality	
	Phae	**Rhod**	**Phae**	**Rhod**	**Phae**	**Rhod**	**Phae**	**Rhod**	**Phae**	**Rhod**	**Phae**	**Rhod**	**Phae**	**Rhod**
R	0.03	**0.39**	0.19	**0.26**	0.12	**0.36**	0.03	**0.38**	-0.02	0.12	-0.05	**0.29**	0.09	**0.37**
p-val	>0.05	0.002	>0.05	0.03	>0.05	0.01	>0.05	0.0008	>0.05	>0.05	>0.05	0.007	>0.05	0.003

Loc = Location, Depth Int = Depth Interval, Host Morph = Host Morphology, Host Branch = Host Branching pattern, Host Annual = Host Annuality. Significant values are highlighted in bold.

https://doi.org/10.1371/journal.pone.0250629.t003

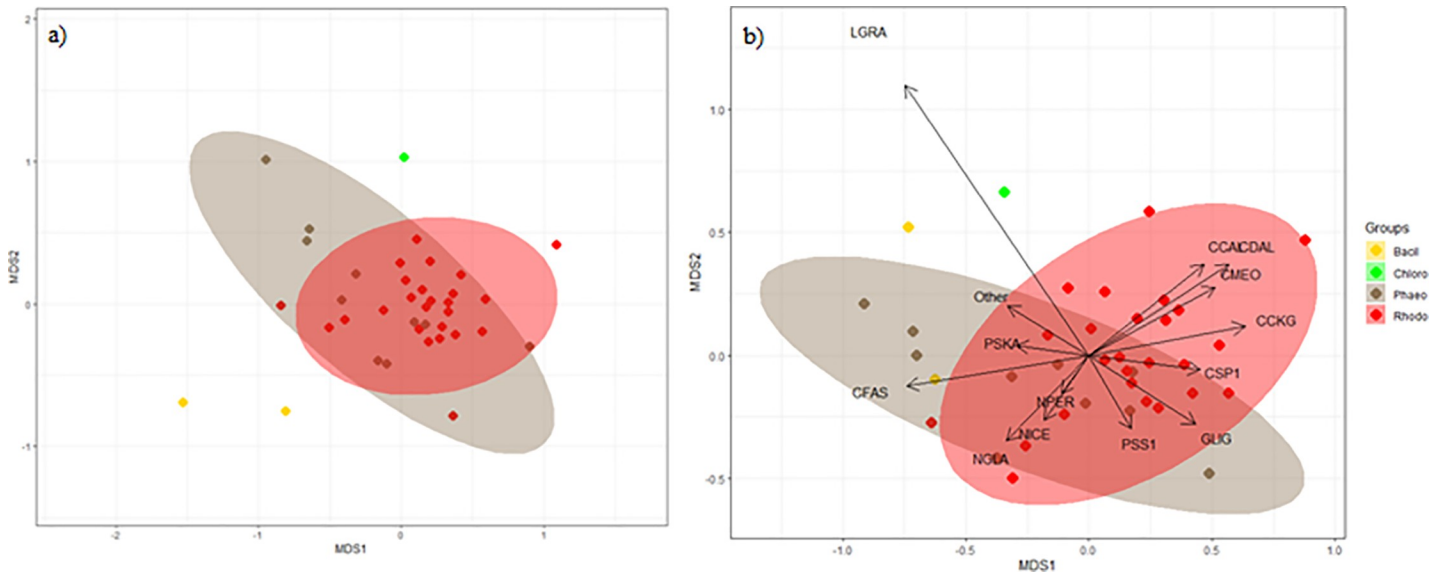

Fig 4. nMDS of the diatom communities. a) complete set and b) predominant diatoms (square root transformed). Bacill = macroscopically visible Bacillariophyceae, Chloro = Chlorophyta, Phaeo = Phaeophyceae, Rhodo = Rhodophyta. Species codes: CCAL = *Cocconeis californica*, CCKG = *Cocconeis californica var. kerguelensis*, CDAL = *Cocconeis dallmanii*, CFAS = *Cocconeis fasciolata*, CMEO = *Cocconeis melchioroides*, CSP1 = *Cocconeis sp. 1*, GLIG = *Gomphonemopsis ligowskii*, LGRA = *Licmophora gracilis*, NGLA = *Navicula glacialis*, NICE = *Navicula incertata*, NPER = *Navicula perminuta*, PSKA = *Pseudogomphonema kamtschaticum*, PSS1 = *Pseudogomphonema sp 1*, Other = diatom species in under 2% frequency and abundance.

https://doi.org/10.1371/journal.pone.0250629.g004

r = 0.299***). The frequency of teratologies found was higher in LI (56.52% of samples had teratological cells, arriving at 2.3% of incidence in a sample) than in DI (66.67% of samples had teratological cells, with an incidence between 0–1% of the samples). However, only samples from Deception island did not arrive to 500 valves due to sparse epiphyte concentration.

Given that we had not enough specimens of macroscopic diatom colonies (n = 2) and Chlorophyta (n = 1), only Rhodophyta and Phaeophyceae samples were considered henceforth. When comparing the depth distribution of predominant diatom taxa (Fig 6), frequent or abundant diatom taxa, or both, differences between the samples from LI and DI became apparent. Larger diatoms, such as *Cocconeis fasciolata* (Ehrenberg) N. E. Brown or *C. antiqua*

Table 4. Average abundance and dissimilarity of diatom communities from Rhodophyta (Rhod) and Phaeophyceae (Phae).

Taxa	Average abundance		Average dissimilarity	SD	Contribution (%)	Cumulated (%)
	Phaes	Rhod				
Navicula perminuta	18.36	15.88	8.48	1.05	11.65	11.65
Gomphonemopsis ligowskii	12.19	8.79	7.42	0.94	10.19	21.84
Cocconeis melchioroides	1.44	13.65	6.48	0.88	8.90	30.73
***Pseudogomphonema* sp. 1**	10.72	12.21	6.44	1.05	8.84	39.58
Cocconeis fasciolata	10.28	0.94	5.13	0.66	7.04	46.61
Pseudogomphonema kamtschaticum	8.80	4.77	4.01	1.09	5.51	52.12
Cocconeis californica var. kerguelensis	0.23	7.38	3.68	0.56	5.05	57.17
Tabularia tabulata	6.80	0.09	3.43	0.32	4.71	61.88
Cocconeis dallmannii	0.92	5.20	2.69	0.62	3.69	65.57
Cocconeis costata	4.94	2.01	2.53	0.73	3.48	69.05
Cocconeis californica	1.21	4.13	2.32	0.47	3.19	72.23

Species ordered in decreasing and cumulated contributions (SIMPER analysis). SD = Standard deviation.

https://doi.org/10.1371/journal.pone.0250629.t004

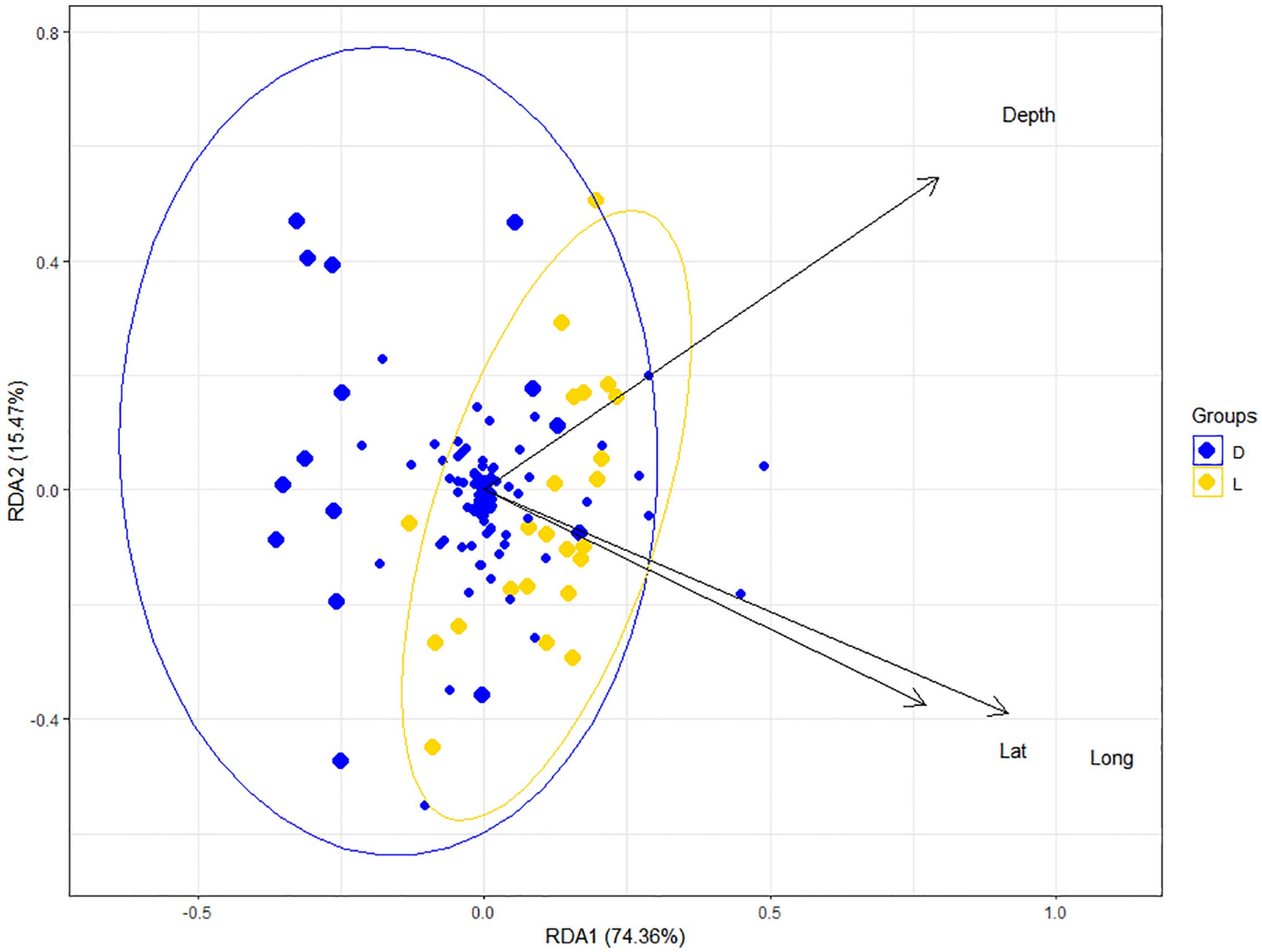

Fig 5. RDA with the first two axes explaining 89.83% of total variance Eigen values of axis 1 = 2.80 and axis 2 = 0.582. DI = Deception island, LI = Livingston island.

https://doi.org/10.1371/journal.pone.0250629.g005

Tempère & Brun, were found on samples located in shallower locations in DI, while smaller diatoms, as *Navicula cf. perminuta* Grunow were mostly found in comparatively deeper samples. On the contrary, in LI, this depth-cell size trend was reversed. The differentiation of diatom communities with respect to sampling depth was significant as well (Mantel statistic $r = 0.260^{***}$).

ANOSIM showed that the importance of factors determining diatom community composition differed between both islands (Table 5). The predominant factor was host algae species on LI ($R = 0.7^{***}$) and depth on DI ($R = 0.54^{***}$). Host class was significant in both locations (DI $R = 0.38^{***}$, LI $R = 0.4^{*}$). SIMPER analysis (Table 6) further showed an average dissimilarity of 70.71% between islands and an intra-island dissimilarity of 59.51% (LI) and 74.80% (DI). The most characteristic diatom species for DI were *Cocconeis melchioroides*, *Pseudogomphonema* sp. 1 and *Gomphonemopsis ligowskii*. In LI, the predominant diatom was *Navicula perminuta*. Both islands had saturated rarefaction curves (S2 Fig), and DI seemed to have the richest diatom community.

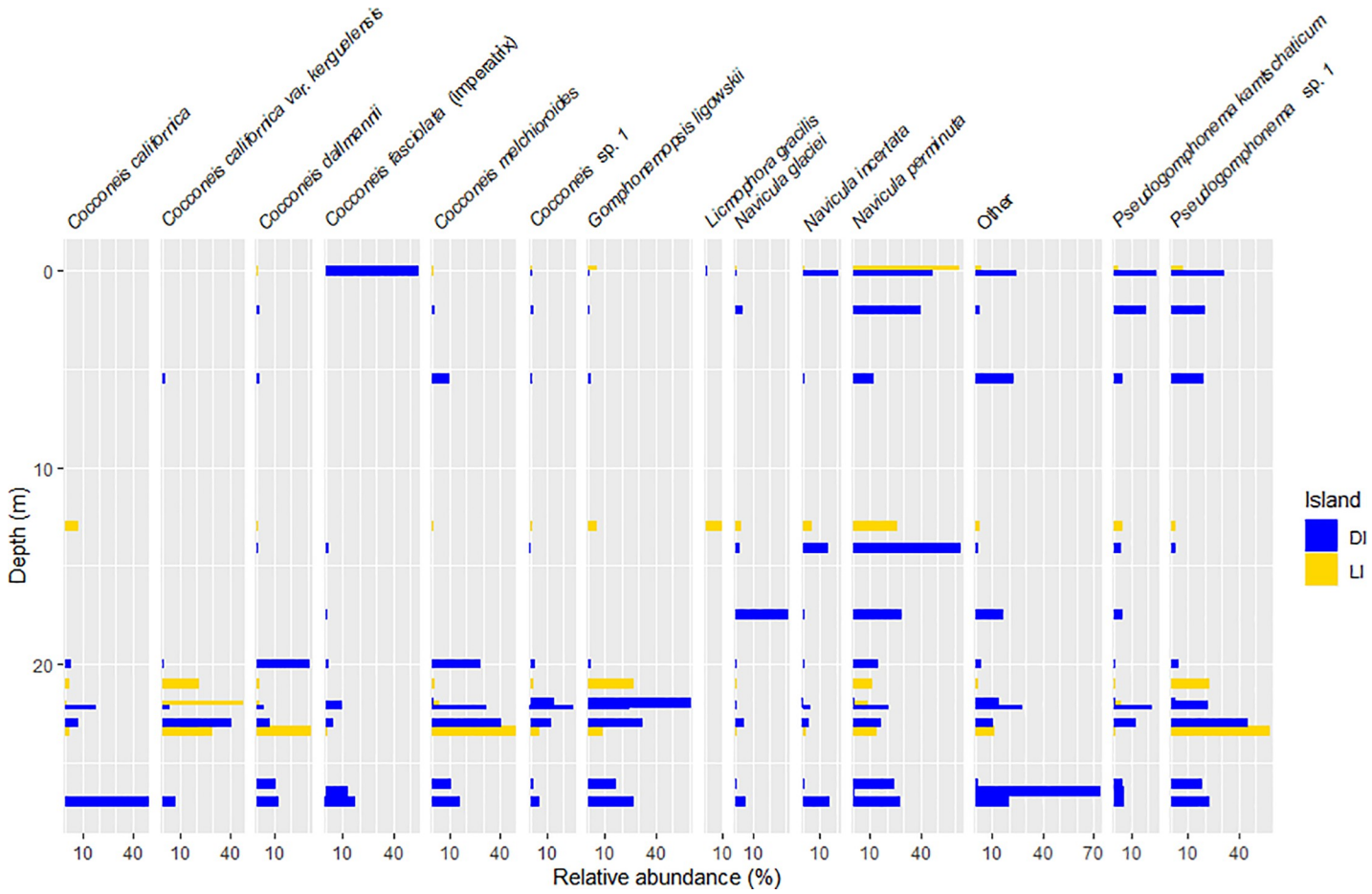

Fig 6. Depth diagram of diatom distribution in Deception and Livingston Island. The rest of diatoms found are summarized in the "Other" panel.

https://doi.org/10.1371/journal.pone.0250629.g006

Antarctic epiphytic diatoms in the literature. A Mantel test on a presence-absence database created from diatom community composition depending on study location showed significance in the richness of the epiphytic diatom communities according to geographical GPS spherical trigonometric distance (Mantel statistic r = 0.4675**). When comparing the diatom composition of the samples, the sample of Vestfold Hills was the most diversified from the rest when comparing epiphytic diatom composition using a hierarchical clustering (Fig 7, S3–S5 Tables). The samples from McMurdo Sound (MS) clustered together, and our samples clustered with the South Shetland Islands (SSI) sample from Potter Cove. The sample from Admiralty Bay, however, clustered with the diatom composition found on macroalgae from MS.

Table 5. ANOSIM test results performed on communities from Deception (DI) and Livingston Island (LI).

	Host algae		Host class		Depth [m]		Year		Host morph.		Host branch		Host annual	
	D	L	D	L	D	L	D	L	D	L	D	L	D	L
R	0.04	**0.70**	**0.38**	**0.40**	**0.54**	0.12	0.26	0.22	0.21	0.13	0.03	0.04	0.15	0.13
p-value	>0.05	0.0001	0.001	0.01	0.008	>0.05	>0.05	>0.05	>0.05	>0.05	>0.05	>0.05	>0.05	>0.05

Significant values are highlighted in bold.

https://doi.org/10.1371/journal.pone.0250629.t005

Table 6. Breakdown of average dissimilarity between epiphytic diatoms in Deception and Livingston Island locations (SIMPER).

Taxa	Average abundance		Average dissimilarity	SD	Contribution (%)	Cumulated (%)
	Deception	Livingston				
Navicula perminuta	16.89	14.90	8.00	1.01	10.44	10.44
Gomphonemopsis ligowskii	6.11	10.91	6.94	0.98	9.05	19.50
***Pseudogomphonema* sp.1**	8.08	12.51	6.39	0.99	8.34	27.83
Cocconeis melchioroides	2.71	13.09	6.37	0.87	8.31	36.14
Cocconeis fasciolata	7.64	0.97	3.91	0.56	5.11	41.25
Cocconeis californica var. kerguelensis	0.83	7.36	3.78	0.57	4.94	46.19
Pseudogomphonema kamtschaticum	6.19	5.54	3.42	1.00	4.46	50.65
Cocconeis californica	3.64	2.48	2.79	0.47	3.64	54.29
Cocconeis dallmannii	0.96	5.22	2.79	0.63	3.64	57.92
Berkeleya rutilans	5.18	0.00	2.60	0.27	3.39	61.31
Tabularia tabulata	5.00	0.09	2.54	0.27	3.31	64.62
Brandinia	4.96	0.01	2.49	0.28	3.25	67.87
Navicula incertata	4.49	1.78	2.24	0.73	2.92	70.79

Species ordered in decreasing and cumulated contributions (SIMPER analysis). SD = standard deviation.

https://doi.org/10.1371/journal.pone.0250629.t006

ANOSIM showed significant differences in diatom composition by study after controlling for geographic effect ($R = 0.78^{***}$), after controlling for geographic effects study made out ($R = 0.81^{***}$). For further characterization, a SIMPER analysis was used following the distribution around Antarctica. Samples from SSI, MS, and Vestfold Hills (VH) showed significant differences among each other, with MS and VH having the highest average dissimilarity (99.51), followed by South Shetland Islands and VH (98.89), and SSI and MS being the lowest (80.54). MS was characterised by the most frequent taxa *Fragilariopsis nana*, *Cocconeis fasciolata* and *Pseudogomphonema kamtschaticum*. In VH only *Nitzschia lecointei* seemed to be characteristic. The most frequent taxa in SSI, which includes the diatoms of our study, were *Navicula perminuta* and *Cocconeis melchioroides*. The comparison of diversity (S6 Table) showed that the DI samples had the highest species richness overall (S = 94) and a relatively high Shannon diversity (H' = 3.16) compared to the other SSI samples (H' = 2.63–2.90). SSI and MS sites had similar values of diversity (H' = 2.63–3.87) and richness (S = 45–118).

Discussion

The total number of taxa identified in this study, 129 species and 44 genera, exceeds the number of taxa in previous Antarctic epiphytic diatom studies. Even after eliminating the diatom samples from the dataset, a total of 120 species and 42 genera of epiphytic diatoms were identified on macroalgal samples, still surpassing the diversity found in previous studies. This could be an effect of a broader sampling along the depth gradient, of a high richness of macroalgal species investigated in this study, or the gentle preparation method used. A partial explanation of high diatom species richness in Antarctic-Subantarctic marine benthos might be the unusually high nutrient concentrations (especially of nitrate) surrounding the Antarctic peninsula [22] in combination with higher iron levels [47]. The high richness of macroalgal species investigated in this study in combination with the ecological niche diversity is, however, probably more important. Majewska et al [3,15] studies were only based on three Rhodophyta taxa. The study on epiphytic diatoms in Vestfold Hills [12] had 17 host species, but epiphytic diatom species numbers remained low as the authors only reported diatoms commonly found on different types of macroalgae and sea ice. The most comparable study would be Al-Handall et al.

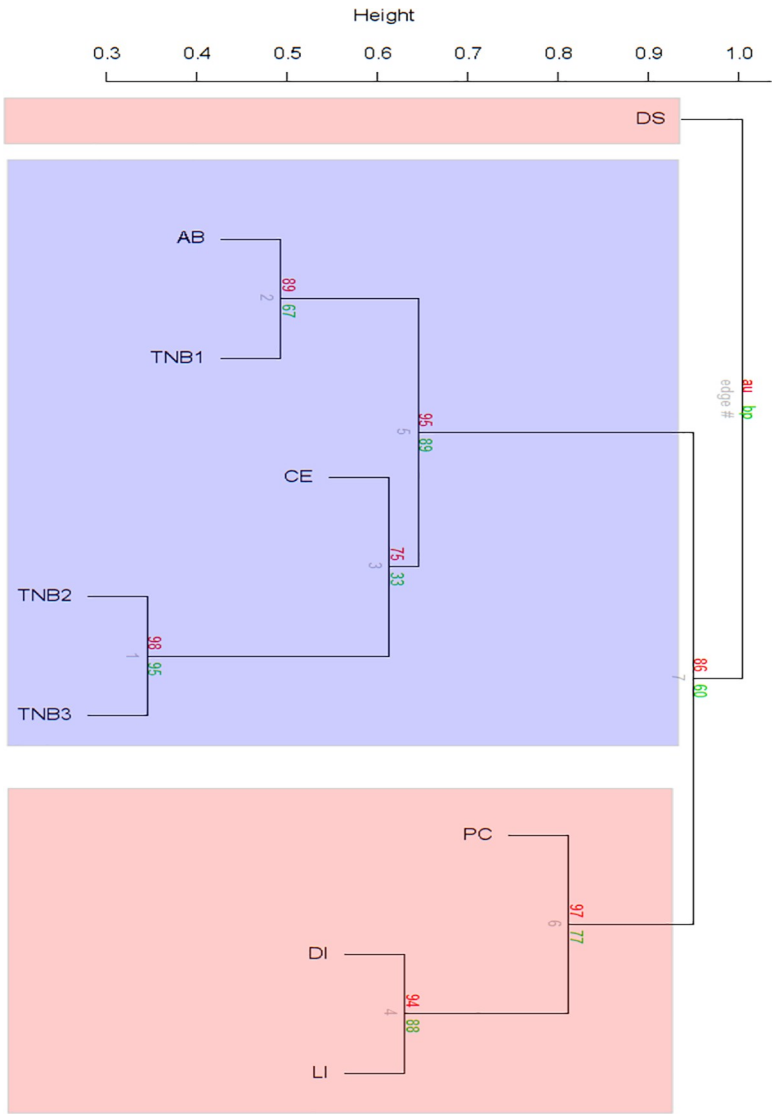

Fig 7. Hierarchical clustering calculated with 10,000 permutations with the studies of Davis Station (DS), Terra Nova Bay (TNB1, 2, 3), and South Shetland Islands (Deception [DI], Livingston [LI], and King George Island, divided into Potter Cove [PC] and Admiralty Bay [AB]) with presence-absence data aggregated at the study level (n total = 192).

https://doi.org/10.1371/journal.pone.0250629.g007

[2] (19 host species and individual samples), which listed 50 species, compared to our total of 20 macrophyte taxa (and 38 samples).

In spite of previous studies, 20 diatom species were recorded for the first time in DI and LI (S1 Table, bold). Most of them pertained to the *Cocconeis* Ehrenberg genus, a monoraphid and mostly epiphytic diatom [48]. This genus was also predominant in previous studies [3,13–15]. One frequent diatom taxon was identified as an unknown species. *Pseudogomphonema* sp. 1 was smaller than *Pseudogomphonema plinskii* Witkowski, Metzelin & Lange-Bertalot and the endophytic diatom found inside the macroalgal genus *Neoabbottiella* [49] and could be yet undescribed. In contrast with the epiphytic diatom studies, usual proxies for sea-ice as *Fragilariopsis curta* [50] and *Thalassiosira antarctica* [51] were not found in as much predominance as, for instance, in Majewska et al. [3].

Epiphytic diatom floristics and ecology

Seaweeds respond to changes in several ways, including by secreting secondary metabolites with antibiotic or antifouling activities on surfaces susceptible to epiphytic invasion [19–21,52]. This could activate the acclimatisation mechanisms of epiphytic diatoms and co-specialization could be prompted. In our study however, the difference between both islands could reflect different taxonomic coverages of sampling, rather than genuine biogeographic signal: whereas most of the samples from LI were Rhodophyta (>82%), in DI the proportions were 40% Rhodophyta and 46% Phaeophyceae. Therefore, the DI samples contained more information on the effect of host at the higher taxonomic level and could be better compared with Al-Handal and Wulff [2], while LI samples more information at lower taxonomic level within red algae, showing more similarities to the Majewska results [3].

Apart from taxonomic identity, also branching pattern and annuality of the host have previously been found to shape epiphyte communities [53]. We found such associations, too, like some species of *Cocconeis* occurring only on branched Rhodophyta hosts (e.g. *Desmarestia* or *Plocamium*), which coincides with findings in other Antarctic and worldwide marine epiphytic diatom studies [3,54–57]. In our study, the effect of branching pattern and annuality was only significant on Rhodophyta and not on Phaeophyceae hosts. As the host age increases, so does the colonization by a mature biofilm community [58]. Maturity of the biofilm, and thus organism position inside a polysaccharide casing, could also protect the community living in it, as shown in several heavy metal studies [59,60]. This might partially explain the annuality effect.

It is instrumental to compare study designs across Antarctic-Subantarctic epiphyte diatom studies. Whereas most sampling campaigns in these distant regions are opportunistic by necessity [2,12], Majewska and collaborators [3,13–15] deliberately focused on three macroalgal host species, systematically capturing epiphyte variability on these selected hosts. In contrast, the present study sampled non-selectively, but the so far broadest diversity of host taxa, and at least some of them repeatedly. Comparing results from both types of approaches, it becomes clear that a systematic and repeated sampling of a broader range of host species will be required for a final clarification of the specificity of host-epiphyte associations. With respect to host-trait effects on epiphyte communities, it would be interesting to more systematically compare branched vs unbranched red and brown seaweed host taxa (for instance the Rhodophyta *Plocamium cartilagineum* vs. *Iridaea chordata*, and the Phaeophyceae *Desmarestia antarctica* vs. *Hymantothallus grandifolius*).

Geographical distribution of diatoms in Antarctica

The total species richness found in DI (93) far exceeded the expectations for an extreme environment, being lower in LI (82). In LI a higher variability in light impact could have been expected because of glacier inputs [61]. Better micronutrient supply due to the volcanic exudations on DI might have increased the number of species [47]. On the other hand, substrate consistency could also have an effect on diatom colonization. The fine (lapilli) consistency in DI causes quickly changing light intensities, since the substrate can quickly redeposit itself after being moved. In contrast, the light influx of LI does not depend on movement of lapilli, but varies due to the input from time constrained glacier melt [62], thus providing more stable irradiation for macroalgae and epiphytic diatoms during the sampled Antarctic summer.

Deception island (DI) is a quiescent volcano, with a semi-submerged cone. The caldera is only 180 m deep [63] and has active hydrothermal vent activity [64]. This has been found to increase the bioavailability of trace elements [65], and also to increase colloid suspension because of the fine sediment or lapilli [64]. The existence of active fumaroles also increases the temperature range measured in the water and substrate [66], thus further segregating potential

ecological niches in the ecosystem. Another important difference between the two islands is that LI has a slightly higher tide amplitude and narrower range of water temperature than Deception island [67].

The difference in diatom taxa of both islands was smaller than expected and also smaller than the host effect. Host species that were sampled in DI and LI once or more were compared between and within locations (*Desmarestia antarctica*, *Gigartina skottsbergii*, *Hymantothallus grandifolius*, *Iridaea cordata* and *Palmaria decipiens*) and showed that the dissimilarity among DI samples was greater than in LI or in comparison between DI and LI. This might point to the environmental variability inside the DI caldera creating more ecological niches for diatom species to fill [68], but unfortunately, physicochemical and light intensity measurements which would be needed to substantiate this are not available.

On a broader geographic scale, similarity of diatom communities around Antarctica was strongly dependent on study. Using presently available data, it is not possible to separate geographic differences from environmental effects and possible effects of methodological differences among studies (further discussed in Closing methodological remarks). It is of course to be seen as a tentative comparison of epiphytic diatom distribution around Antarctica, since other variables concerning seasonality and physicochemical composition of the waters in each of the studies was mostly unavailable and further, synchronous studies should be made to answer the question of epiphytic diatom biogeography around Antarctica. This study would be a first approach, but as discussed, new and more standardized / synchronised efforts should be made in the future to obtain a clear picture on the ecological variations of epiphytic diatoms along the Antarctic coastline.

Closing methodological remarks

One of the most striking observations of our study was the strong effect of study upon epiphytic diatom communities. As discussed above, the exact cause of this study effect is difficult to pin down based on presently available data, but preparation method might be part of it. The dehydration method used by Majewska and collaborators [3,5,13–15] permitted a quantitative in situ observation but could potentially lead to overlooking taxa growing in lower layers of the established biofilm on the host algae. As previously discussed by Majewska et al [3], the reduced diatom species richness in Al-Handal & Wulff [2] and Thomas & Jiang [12] could be an effect of dissolution of lightly silicified frustules. Although silicate is known to dissolve faster in alkaline than in acidic milieu, Carr [25] and Friedrichs [24] found that a short-time bleach treatment, as used in this study, is more gentle to diatom frustules than commonly applied harsh oxidizing acid treatments which was used by previous ones. Parallel preparations from the same sample using both types of approaches in the future would be useful to test whether the effect of preparation treatment is indeed the dominant cause of study effect. Once this has been clarified, a clearer recommendation for standardizing the methodology of epiphytic diatom preparation can be given which will be important to improve the comparability of results among different studies.

Another methodological difference of our study from previous ones was the use of virtual slide microscopy and web-based manual taxonomic annotation. We did not systematically test this effect in these studies, but checking individual samples both on the light microscope and in the slide scans indicates that this is not causing a major bias for observing taxonomic composition (a study systematically comparing this effect is presently in preparation). We think that this methodology has some potential advantages for the future. For instance, a digital image of every single frustule identified in this study is available in PANGAEA (doi: https://doi.pangaea.de/10.1594/PANGAEA.925913). Future studies making literature comparisons,

like attempted also above, will thus not only have presence-absence records, but also every one of these images, making it even possible to re-identify any or all frustules as deemed necessary. This can, in the long run, when such data sets accumulate, contribute a lot to transparency and comparability among different studies.

In conclusion, in this study we compared epiphytic diatom communities living on several macroalgae in Deception and Livingston Island. We found that the number of species in DI samples exceeded those from LI and from previous studies. The former observation may point to a higher proportion of niches found on the volcanic island. The second one would be explained by a gentler preparation method, though this needs a clear causal confirmation in the future.

Supporting information

S1 Fig. Rarefaction curves of macrophytes hosts. Rhodo = Rhodophyta, phaeo = Phaeophyceae, bacil = Bacillariophyceae, chloro = Chlorophyta.
(TIF)

S2 Fig. Rarefaction curves of sample location in this study. Dec = Deception island, Liv = Livingston island.
(TIF)

S1 Table. Epiphytic diatom composition and frequency on Antarctic macroalgae, specific proportion and occurrence on Deception (DI) and Livingston Island (LI). Pheaophyceae (Phaeo, n = 10), Rhodophyta (Rhodo, n = 25), Bacillariophyceae (Bac, n = 2) and Chlorophytas (Chlo, n = 1) have been investigated. Macroalgal host: Au = *Adenocystis utricularis*, Bc = *Ballia callitricha*, Cj = *Cystosphaera jacquinotii*, Dp = *Delisea pulchra*, Dan = *Desmarestia anceps*, Dant = *Desmarestia antarctica*, Ds = *Desmarestia sp*., Gs = *Gigartina skottsbergii*, Gt = *Gymnogongrus turquettii*, Hg = *Himantothallus grandifolius*, Ic = *Iridaea cordata*, Mh = *Monostroma hariotii*, Mm = *Myriogramme cf. manginii*, Pd = *Palmaria decipiens*, Pp = *Piccionella plumosa*, Pc = *Plocamium cartilagineum*, Ph = *Plocamium cf. hookeri*, Pe = *Pyropia endiviifolia*. Bold text shows first records in DI and LI.
(DOCX)

S2 Table. SIMPER analysis of comparison of predominant diatom species in LI and DI.
(DOCX)

S3 Table. SIMPER analysis of comparison of epiphytic diatom communities in the South Shetland Islands (SSI, n = 4) and Vestfold Hills (VH, n = 1).
(DOCX)

S4 Table. SIMPER analysis of comparison of diatom communities in the South Shetland Islands (SSI, n = 4) and MacMurdo Sound (MMS, n = 4).
(DOCX)

S5 Table. SIMPER analysis of comparison of epiphytic diatom communities in the Vestfold Hills (VH, n = 1) and MacMurdo Sound (MMS, n = 4).
(DOCX)

S6 Table. Diversity/Entropy indices of the compared studies. * = contains only macroalgal information, not Bacillariophyceae. | = total data of the study.
(DOCX)

S7 Table. Mantel result comparison of parameters and diatom abundance.
(DOCX)

Acknowledgments

We would like to thank all the scientists involved in sampling Antarctic macroalgae, particularly Elisenda Ballesté and Blanca Figuerola. Special thanks are also given to both Spanish Research Stations crews for their help in the summer cruises 2017–2019, as well as the ship-s'crews of Bio-Hespérides and Sarmiento de Gamboa for logistic support. We also acknowledge Quantarctica and the Norwegian Polar Institute for the use of the Quantarctica maps created for this paper. This study is part of the SCAR-Biology Programme–State of the Antarctic Ecosystem (AntEco: https://www.scar.org/science/anteco/home).

Author Contributions

Conceptualization: Andrea M. Burfeid-Castellanos, Rafael P. Martín-Martín.

Data curation: Andrea M. Burfeid-Castellanos, Michael Kloster.

Formal analysis: Andrea M. Burfeid-Castellanos, Carlos Angulo-Preckler, Bánk Beszteri.

Funding acquisition: Andrea M. Burfeid-Castellanos, Conxita Avila.

Investigation: Rafael P. Martín-Martín, Conxita Avila, Bánk Beszteri.

Methodology: Andrea M. Burfeid-Castellanos, Michael Kloster.

Project administration: Andrea M. Burfeid-Castellanos, Conxita Avila.

Resources: Bánk Beszteri.

Supervision: Bánk Beszteri.

Validation: Andrea M. Burfeid-Castellanos, Carlos Angulo-Preckler.

Writing – original draft: Andrea M. Burfeid-Castellanos.

Writing – review & editing: Andrea M. Burfeid-Castellanos, Rafael P. Martín-Martín, Michael Kloster, Carlos Angulo-Preckler, Conxita Avila, Bánk Beszteri.

References

1. McMinn A, Pankowskii A, Ashworth C, Bhagooli R, Ralph P, Ryan K. In situ net primary productivity and photosynthesis of Antarctic sea ice algal, phytoplankton and benthic algal communities. Marine Biology. 2010; 157:1345–56. https://doi.org/10.1007/s00227-010-1414-8
2. Al-Handal AY, Wulff A. Marine epiphytic diatoms from the shallow sublittoral zone in Potter Cove, King George Island, Antarctica. Botanica Marina. 2008; 51:411–35. https://doi.org/10.1515/BOT.2008.053
3. Majewska R, Convey P, Stefano M de. Summer epiphytic diatoms from terra nova bay and cape evans (Ross Sea, Antarctica)—A synthesis and final conclusions. PLoS ONE. 2016; 11:1–30. https://doi.org/10.1371/journal.pone.0153254 PMID: 27078637
4. Totti CM, Poulin M, Romagnoli T, Perrone C, Pennesi C, Stefano M de. Epiphytic diatom communities on intertidal seaweeds from Iceland. Polar Biology. 2009; 32:1681–91. https://doi.org/10.1007/s00300-009-0668-4
5. Majewska R, Gambi MC, Totti CM, Pennesi C, Stefano M de. Growth form analysis of epiphytic diatom communities of Terra Nova Bay (Ross Sea, Antarctica). Polar Biology. 2013; 36:73–86. https://doi.org/10.1007/s00300-012-1240-1
6. Wahl M. Marine epibiosis. I. Fouling and Antifouling: Some Basic Aspects. Marine Ecology Progress Series. 1989; 58:175–89.
7. Sand-Jensen K. Effect of epiphytes on eelgrass photosynthesis. Aquatic Botany. 1977; 3:55–63. https://doi.org/10.1016/0304-3770(77)90004-3
8. Montes-Hugo M, Doney SC, Ducklow HW, Fraser W, Martinson D, Stammerjohn SE, et al. Recent Changes in Phytoplankton Communities Associated with Rapid Regional Climate Change Along the Western Antarctic Peninsula. Science. 2009; 323:1470–3. https://doi.org/10.1126/science.1164533 PMID: 19286554.

9. Pellizzari F, Silva MC, Silva EM, Medeiros A, Oliveira MC, Yokoya NS, et al. Diversity and spatial distribution of seaweeds in the South Shetland Islands, Antarctica: an updated database for environmental monitoring under climate change scenarios. Polar Biology. 2017; 40:1671–85. https://doi.org/10.1007/s00300-017-2092-5

10. Hughes KA, Pescott OL, Peyton J, Adriaens T, Cottier-Cook EJ, Key G, et al. Invasive non-native species likely to threaten biodiversity and ecosystems in the Antarctic Peninsula region. Global Change Biology. 2020; 26:2702–16. https://doi.org/10.1111/gcb.14938 PMID: 31930639

11. Avila C, Angulo-Preckler C, Martín-Martín RP, Figuerola B, Griffiths HJ, Waller CL. Invasive marine species discovered on non–native kelp rafts in the warmest Antarctic island. Scientific Reports. 2020; 10:1639. https://doi.org/10.1038/s41598-020-58561-y PMID: 32005904

12. Thomas DP, Jiang J. Epiphytic diatoms of the inshore marine area near Davis Station. Hydrobiologia. 1986; 140:193–8. https://doi.org/10.1007/BF00007435

13. Majewska R, Gambi MC, Totti CM, Stefano M de. Epiphytic diatom communities of Terra Nova Bay, Ross Sea, Antarctica: Structural analysis and relations to algal host. Antarctic Science. 2013; 25:501–13. https://doi.org/10.1017/S0954102012001101

14. Majewska R, Stefano M de. Epiphytic diatom communities on *Phyllophora antarctica* from the Ross Sea. Antarctic Science. 2014; 13:1–13. https://doi.org/10.1017/S0954102014000327

15. Majewska R, Kuklinski P, Balazy P, Yokoya NS, Paternostro Martins A, Stefano M de. A comparison of epiphytic diatom communities on *Plocamium cartilagineum* (*Plocamiales, Florideophyceae*) from two Antarctic areas. Polar Biology. 2015; 38:189–205. https://doi.org/10.1007/s00300-014-1578-7

16. Da Ferreira Silva J, Oliveira Linton MA, Da Ribeiro Anunciação R, Da Pereira Silva E, Alves RP, Schünemann AL, et al. Distribution of aerophilous diatom communities associated with terrestrial green macroalgae in the South Shetland Islands, Maritime Antarctica. PLoS ONE. 2019; 14:e0226691. https://doi.org/10.1371/journal.pone.0226691 PMID: 31887164

17. Rosado B, Fernández-Ros A, Berrocoso M, Prates G, Gárate J, Gil A de, et al. Volcano-tectonic dynamics of Deception Island (Antarctica): 27 years of GPS observations (1991–2018). Journal of Volcanology and Geothermal Research. 2019; 381:57–82. https://doi.org/10.1016/j.jvolgeores.2019.05.009

18. Vieira G, Lopez-Martinez J, Serrano E, Ramos M, Gruber S, Hauck C, et al. Geomorphological observations of permafrost and ground-icedegradation on Deception and Livingston islands, maritime Antarctica. 9th International Conference on Permafrost. Fairbanks, Alaska; 2008. pp. 1839–44.

19. Gómez I, Huovinen P, editors. Antarctic Seaweeds: Diversity, Adaptation and Ecosystem Services. Cham: Springer International Publishing; 2020.

20. Wiencke C, Amsler CD, Clayton MN. Chapter 5.1. Macroalgae. In: Broyer C de, Koubbi P, Griffiths HJ, Raymond B, Udekem d'Acoz Cd, et al., editors. Biogeographic Atlas of the Southern Ocean. Cambridge: Scientific Committee on Antarctic Research.; 2014. pp. 66–73.

21. Wiencke C, Clayton MN. Antarctic seaweeds. Synopses of the Antarctic benthos. ARG Gantner Verlag KG, Ruggell, Lichtenstein; 2002.

22. Zacher K, Rautenberger R, Hanelt D, Wulff A, Wiencke C. 2. The abiotic environment of polar marine benthic algae. De Gruyter; 2010.

23. Vettorato B, Laudares-Silva R, Talgatti D, Menezes M. Evaluation of the sampling methods applied to phycoperiphyton studies in the Ratones River estuary, Brazil. Acta. 2010; 22:257–66. https://doi.org/10.4322/actalb.02203002

24. Friedrichs L. A simple cleaning and fluorescent staining protocol for recent and fossil diatom frustules. Diatom research. 2013; 28:317–27. https://doi.org/10.1080/0269249X.2013.799525

25. Carr JM, Hengenrader GL, Troelstrup NH. A Simple, Inexpensive Method for Cleaning Diatoms Author. Transactions of the American Microscopical Society. 1986; 105:152–7.

26. Kloster M, Esper O, Kauer G, Beszteri B. Large-Scale Permanent Slide Imaging and Image Analysis for Diatom Morphometrics. Applied Sciences. 2017; 7:330. https://doi.org/10.3390/app7040330

27. Schindelin J, Arganda-Carreras I, Frise E, Kaynig V, Longair M, Pietzsch T, et al. Fiji: an open-source platform for biological-image analysis. Nature Methods. 2012; 9:676–82. https://doi.org/10.1038/nmeth.2019 PMID: 22743772

28. Blattner T, Stivalet B, Keyrouz W, Brady M, Chalfoun J, Zhou S. A Hybrid CPU-GPU System for Stitching of Large Scale Optical Microscopy Images. 2014: 9.

29. Chalfoun J. A power stitching tool. SPIE Newsroom. 2014. https://doi.org/10.1117/2.1201402.005365

30. Chalfoun J, Majurski M, Blattner T, Bhadriraju K, Keyrouz W, Bajcsy P, et al. MIST: Accurate and Scalable Microscopy Image Stitching Tool with Stage Modeling and Error Minimization. Scientific Reports. 2017; 7:1–10. https://doi.org/10.1038/s41598-016-0028-x PMID: 28127051

31. Preibisch S, Saalfeld S, Tomancak P. Globally optimal stitching of tiled 3D microscopic image acquisitions. Bioinformatics. 2009; 25:1463–5. https://doi.org/10.1093/bioinformatics/btp184 PMID: 19346324.

32. Langenkämper D, Zurowietz M, Schoening T, Nattkemper TW. BIIGLE 2.0—Browsing and Annotating Large Marine Image Collections. Frontiers in Marine Science. 2017; 4. https://doi.org/10.3389/fmars.2017.00083

33. Medlin LK, Priddle J. Polar marine diatoms. Cambridge: British Antarctic Survey; 1990. https://doi.org/10.7748/ns.5.3.42.s48 PMID: 27652656

34. Scott FJ, Marchant HJ. Antarctic marine protists. Canberra: Australian Biological Resources Study; 2005.

35. Falasco E, Bona F, Badino G, Hoffmann L, Ector L. Diatom teratological forms and environmental alterations: a review. Hydrobiologia. 2009; 623:1–35. https://doi.org/10.1007/s10750-008-9687-3

36. Shannon CE, Weaver W. The Mathematical Theory of Communication.; 1964.

37. R Development Core Team. R: A language and environment for statistical computing. Vienna, Austria.: R Foundation for Statistical Computing; 2008.

38. Team RStudio. RStudio: Integrated Development for R. RStudio, Inc., Boston, MA; 2015.

39. Legendre P, Legendre L. Numerical Ecology. 3rd ed. Elsevier Science B.V; 2003.

40. Hamilton N. Package 'ggtern'. R topics documenter; 2020.

41. Oksanen J. Multivariate Analysis of Ecological Communities in R.; 2013.

42. Maechler M, Struyf A, Hubert M, Hornik K, Studer M, Roudier P. Package 'cluster'.; 2015.

43. Suzuki R, Shimodaira H. Package 'pvclust'.; 2015.

44. Hijmans RJ, Williams E, Vennes C. Package 'geosphere'; 2019.

45. QGIS Development Team. QGIS Geographic Information System. Open Source Geospatial Foundation Project; 2009.

46. Roth G, Matsuoka K, Skoglund A, Melvær Y, Tronstad S. Quantarctica: A Unique, Open, Standalone GIS Package for Antarctic Research and Education. EGU General Assembly Conference Abstracts. 2017:1973.

47. Bendia AG, Signori CN, Franco DC, Duarte RTD, Bohannan BJM, Pellizari VH. A Mosaic of Geothermal and Marine Features Shapes Microbial Community Structure on Deception Island Volcano, Antarctica. Front Microbiol. 2018; 9:899. Epub 2018/05/07. https://doi.org/10.3389/fmicb.2018.00899 PMID: 29867810.

48. Romero OE, Rivera P. Morphology and Taxonomy of Three Varieties of *Cocconeis costata* and *C. pinnata* (*Bacillariophyceae*) with Considerations of Pleuroneis. Diatom research. 1996; 11:317–43. https://doi.org/10.1080/0269249X.1996.9705388

49. Klochkova TA, Pisareva NA, Park JS, Lee JH, Han JW, Klochkova NG, et al. An endophytic diatom, *Pseudogomphonema* sp. (*Naviculaceae, Bacillariophyceae*), lives inside the red alga *Neoabbottiella* (*Halymeniaceae*, Rhodophyta). Phycologia. 2014; 53:205–14. https://doi.org/10.2216/13-229.1

50. Gersonde R, Zielinski U. The reconstruction of late Quaternary Antarctic sea-ice distribution—the use of diatoms as a proxy for sea-ice. Palaeogeography, Palaeoclimatology, Palaeoecology. 2000; 162:263–86. https://doi.org/10.1016/S0031-0182(00)00131-0

51. Pike J, Crosta X, Maddison EJ, Stickley CE, Denis D, Barbara L, et al. Observations on the relationship between the Antarctic coastal diatoms *Thalassiosira antarctica* Comber and *Porosira glacialis* (Grunow) Jørgensen and sea ice concentrations during the late Quaternary. Marine Micropaleontology. 2009; 73:14–25. https://doi.org/10.1016/j.marmicro.2009.06.005

52. Gómez-Ocampo I. Flora Marina Antártica. Patrimonio de la humanidad. Kultrún; 2016.

53. Wiencke C, Rahmel J, Karsten U, Weykam G, Kirst GO. Photosynthesis of Marine Macroalgae from Antarctica: Light and Temperature Requirements. Botanica Acta. 1993; 106:78–87. https://doi.org/10.1111/j.1438-8677.1993.tb00341.x

54. Al-Handal AY, Riaux-Gobin C, Romero OE, Wulff A. Two New Marine Species of the Diatom Genus *Cocconeis* Ehrenberg: *C. melchioroides* sp. nov. and *C. dallmannii* sp. nov. From King George Island, Antarctica. Diatom research. 2008; 23:269–81. https://doi.org/10.1080/0269249X.2008.9705758

55. Al-Handal AY, Riaux-Gobin C, Wulff A. *Cocconeis pottercovei* sp. nov. and *Cocconeis pinnata var. matsii* var. nov., Two New Marine Diatom Taxa From King George Island, Antarctica. Diatom research. 2010; 25:1–11. https://doi.org/10.1080/0269249X.2010.9705825

56. Car A, Witkowski A, Dobosz S, Burfeind DD, Meinesz A, Jasprica N, et al. Description of a new marine diatom, *Cocconeis caulerpacola* sp. nov. (*Bacillariophyceae*), epiphytic on invasive *Caulerpa* species. European Journal of Phycology. 2012; 47:433–48. https://doi.org/10.1080/09670262.2012.735255

57. García ML, Echazú DM, Romero OE, Maidana NI. *Cocconeis neuquina* Frenguelli (*Bacillariophyta*): emended description, lectotypification, ecology, and geographical distribution. Diatom research. 2018; 33:219–28. https://doi.org/10.1080/0269249X.2018.1485596

58. Desrosiers C, Leflaive J, Eulin A, Ten-Hage L. Optimal colonization and growth of marine benthic diatoms on artificial substrata: protocol for a routine use in bioindication. J Appl Phycol. 2014; 26:1759–71. https://doi.org/10.1007/s10811-013-0204-3

59. Ivorra Castellà N. Metal Induced Succession in Benthic Diatom Consortia. PhD Thesis, Doctoral Thesis. University of Amsterdam. Netherlands. 2000.

60. Duong TT, Morin S, Coste M, Herlory O, Feurtet-Mazel A, Boudou A. Experimental toxicity and bioaccumulation of cadmium in freshwater periphytic diatoms in relation with biofilm maturity. Science of the Total Environment. 2010; 408:552–62. https://doi.org/10.1016/j.scitotenv.2009.10.015 PMID: 19896161.

61. Isla E, Gerdes D, Palanques A, Teixidó N, Arntz W, Puig P. Relationships between Antarctic coastal and deep-sea particle fluxes: implications for the deep-sea benthos. Polar Biology. 2005; 29:249. https://doi.org/10.1007/s00300-005-0046-9.

62. Isla E, Palanques A, Alvà V, Puig P, Guillén J. Fluxes and composition of settling particles during summer in an Antarctic shallow bay of Livingston Island, South Shetlands. Polar Biology. 2001; 24:670–6. https://doi.org/10.1007/s003000100267

63. Cranmer TL, Ruhl HA, Baldwin RJ, Kaufmann RS. Spatial and temporal variation in the abundance, distribution and population structure of epibenthic megafauna in Port Foster, Deception Island. Deep Sea Research Part II: Topical Studies in Oceanography. 2003; 50:1821–42. https://doi.org/10.1016/S0967-0645(03)00093-6

64. Somoza L, Martínez-Frías J, Smellie JL, Rey J, Maestro A. Evidence for hydrothermal venting and sediment volcanism discharged after recent short-lived volcanic eruptions at Deception Island, Bransfield Strait, Antarctica. Marine Geology. 2004; 203:119–40. https://doi.org/10.1016/S0025-3227(03)00285-8

65. Deheyn DD, Gendreau P, Baldwin RJ, Latz MI. Evidence for enhanced bioavailability of trace elements in the marine ecosystem of Deception Island, a volcano in Antarctica. Marine Environmental Research. 2005; 60:1–33. https://doi.org/10.1016/j.marenvres.2004.08.001 PMID: 15649525

66. Berrocoso M, Prates G, Fernández-Ros A, Peci LM, Gil A de, Rosado B, et al. Caldera unrest detected with seawater temperature anomalies at Deception Island, Antarctic Peninsula. Bulletin of Volcanology. 2018; 80:1–12. https://doi.org/10.1007/s00445-018-1216-2

67. Vidal J, Berrocoso M, Fernández-Ros A. Study of tides and sea levels at Deception and Livingston islands, Antarctica. Antarctic Science. 2012; 24:193–201. https://doi.org/10.1017/S095410201100068X

68. Angulo-Preckler C, Figuerola B, Núñez-Pons L, Moles J, Martín-Martín R, Rull-Lluch J, et al. Macrobenthic patterns at the shallow marine waters in the caldera of the active volcano of Deception Island, Antarctica. Continental Shelf Research. 2018; 157:20–31. https://doi.org/10.1016/j.csr.2018.02.005